Numerical simulation of NOx formation in a model gas turbine combustor

Guo, Hongsheng; Liu, Fengshan; Smallwood, Gregory J.; Matovic, Darko

Publisher's version / Version de l'éditeur:

American Flame Research Committee. Spring MeetingAmerican Flame Research Committee 2002 Spring Meeting, pp. 1-11, 2003

MARIA CLANCY
DGO
INST FOR CHEM PROCESS & ENVIR TECH
NATIONAL RESEARCH COUNCIL CANADA
M-12, ROOM 141, 1200 MONTREAL RD.
OTTAWA, ON K1A 0R6
CANADA

ORDER NUMBER:	**CT-07782496-5**
Account Number:	WR001844
Delivery Mode:	XLB
Delivery Address:	
Submitted:	2009/03/04 09:37:17
Received:	2009/03/04 09:37:17
Printed:	2009/03/09 09:57:52

Extended	**Book**	**Internet - transcribed**	**CANADA**

Client Number:	MARIA CLANCY MARCH 2, 2009 # 62
Title:	**AFRC 2002 SPRING MEETING**
Author:	GUO, H.; LIU, F.; SMALLWOOD, G.J.; ET AL
Vol./Issue:	MAY 5-8
Date:	2002
Article Title:	NUMERICAL SIMULATION OF NOX EMISSION IN A MODEL GAS TURBULENT COMBUSTOR

Estimated cost for this 11 page document: $0 document supply fee + $0 copyright = $0

Numerical Simulation of NO_X Formation in a Model Gas Turbine Combustor

Hongsheng Guo, Fengshan Liu, and Gregory J. Smallwood
Combustion Research Group
National Research Council of Canada
Building M-9, 1200 Montreal Road
Ontario, Canada K1A 0R6
Email: hongsheng.guo@nrc.ca

Darko Matovic
Department of Mechanical Engineering
Queen's University
Kingston, Ontario, Canada K7L 3N6

ABSTRACT

NOx formation in a model gas turbine combustor has been numerically investigated using the stretched laminar flamelet model that can deal with finite chemistry. Based on a counterflow non-premixed flame configuration, the flamelet library was created by a detailed chemistry, which consists of 50 species and 312 reactions, and complex thermal and transport properties. The library was then used in a general purpose 3-D flow code FLEX, employing the $k-\varepsilon-Z-g$ turbulence/mixing model.

The simulation results indicate that both NO and N_2O are produced in the higher flame temperature region, while NO_2 is, however, produced near the combustor wall region, where the temperatures are relatively low. The concentration of NO is about two orders of magnitude of that of NO_2, and three orders of magnitude of that of N_2O.

INTRODUCTION

Environmental aspects have been becoming more and more important in the development of various combustion devices. Especially NOx emission will have to be reduced in the future, which has further motivated a great deal of research interest in modeling the characteristics of NO_X emission in practical combustion process. Due to the safety requirements, non-premixed combustors are usually used in practice. Therefore it is of great interest to develop a kind of effective strategy to model NO_X emission process in various combustion devices using non-premixed combustion.

Prediction of NO_X emission in non-premixed turbulent combustion is a complex issue involving many aspects, such as turbulence, variable-density flow, turbulence-chemistry interaction, finite-rate chemical kinetics, differential diffusion and radiative heat transfer etc. Most of commonly used models reduce the phenomenon to a tractable form by introducing drastic simplifying assumptions. The two most popular models are the conserved scalar approach

and eddy-dissipation model (EDM) [1, 2], as implemented in most commercial codes (such as FLUENT, CFX etc.). The key assumptions of this kind of models are fast and equilibrium chemistry. While this kind of models can give relatively reasonable distributions of temperature and some main chemical species in a lot of cases, they feature several limitations due to the restrictive assumptions. The most serious limitation is the equilibrium chemistry, which has been proved to be very crude in predicting the species characterized by comparatively slow chemical kinetics. Among them are carbon monoxide (CO) and NO_X that are closely related to the super-equilibrium concentrations of some minor radicals, such as OH and O.

Considerable attention has been devoted in recent years to the development of models allowing for finite-rate chemistry effects [3]. One of these models is the stretched laminar flamelets [4]. It assumes that a turbulent flame consists of thin laminar flamelets that are convected and stretched by turbulence. As the flamelet structure can be defined by detailed chemical kinetics and complex thermal and transport properties of the reacting species, this approach introduces these effects into the description of turbulent flames.

In the present paper the numerical simulation of NO_X emission in a model gas turbine combustor was conducted by the stretched laminar flamelet model. Based on a counterflow non-premixed flame configuration, the flamelet library was created by a detailed chemistry, which consists of 50 species and 312 reactions, and complex thermal and transport properties. The library was then used in a general purpose 3-D flow code (FLEX), employing the $k-\varepsilon-Z-g$ turbulence/mixing model.

NUMERICAL METHODS

Flamelet Model

Flamelet model assumes that a turbulent flame consists of thin reacting laminar flamelets that are convected and stretched by turbulence. It is based on recasting the conservation equations for scalars by adopting the conserved scalar Z, mixture fraction, as a coordinate through the instantaneous flame front [4]. The stretching action of the flow field on the laminar flamelets is accounted for by introducing the scalar dissipation rate χ, defined as

$$\chi = 2D\frac{\partial Z}{\partial x_k}\frac{\partial Z}{\partial x_k} \tag{1}$$

where D is the molecular diffusivity of Z. As the above coordinate transformation was performed near the flame front, χ must be evaluated either at the stoichiometric location or the maximum flame temperature location. In this paper, the maximum temperature location was used (χ_{max}).

Then the instantaneous value of any state quantity ϕ can be expressed as:

$$\phi = \phi(Z;\chi_{max}) \tag{2}$$

This equation indicates that for any flamelet subjected to a given χ_{max}, the value of ϕ is uniquely related to the mixture fraction Z. It can be obtained from the flamelet library established experimentally or numerically. The corresponding mean value was obtained by introducing the bivariate pdf, $P(Z, \chi_{max})$, as

$$\bar{\phi} = \int_0^\infty \int_0^1 \phi(Z;\chi_{\max}) P(Z,\chi_{\max}) dZ d\chi_{\max} \tag{3}$$

Experimentally and numerically based evidence has indicated that conserved scalar and scalar dissipation rate are statistically independent [4, 5]. Therefore the bivariate pdf can be split into the product of two one dimensional pdfs of a single variable:

$$P(Z,\chi_{\max}) = P(Z)P(\chi_{\max}) \tag{4}$$

Then the integration for the mean value can be written as:

$$\bar{\phi} = \int_0^\infty P(\chi_{\max}) \int_0^1 \phi(Z;\chi_{\max}) P(Z) dZ d\chi_{\max} \tag{5}$$

The pdf of the conserved scalar Z was assumed to have the general form of beta function. It may be written as:

$$P(Z) = \frac{Z^{\alpha-1}(1-Z)^{\beta-1}}{\int_0^1 Z^{\alpha-1}(1-Z)^{\beta-1} dZ} \tag{6}$$

The exponents α and β were given by [5]

$$\alpha = \bar{Z}\left\{\frac{\bar{Z}\left(1-\bar{Z}\right)}{\bar{g}^2} - 1\right\} \tag{7}$$

$$\beta = \frac{(1-\bar{Z})\alpha}{\bar{Z}} \tag{8}$$

Quantities $\bar{Z}$ and $\bar{g}$ are respectively the mean mixture fraction and its variance. They were obtained from the solution of the flow field governing equations (see below).

For the scalar dissipation rate, a log-normal distribution was adopted. It can be written as

$$P(\chi_{\max}) = \frac{1}{\sqrt{2\pi}} \frac{1}{\sigma\chi_{\max}} \exp\left[-\frac{1}{2\sigma^2}\left(\ln \chi_{max} - \mu\right)^2\right] \tag{9}$$

where $\sigma^2 = 2.0$ [4] was adopted, while μ was obtained through the following equation:

$$\bar{\chi} = \exp\left(\mu + \frac{1}{2}\sigma^2\right) \tag{10}$$

with $\bar{\chi}$ being the mean scalar dissipation rate obtained by

$$\overline{\chi} = C_{\chi} \frac{\overline{\varepsilon}}{\overline{k}} \overline{g} \tag{11}$$

Quantities $\overline{k}$ and $\overline{\varepsilon}$ are respectively the turbulent kinetic energy and its viscous dissipation rate, which were obtained by solving the standard $k \sim \varepsilon$ equations. A constant value of 2.0 was used for C_{χ} [4].

Flamelet Library

The flamelet library was obtained through the simulations of a series of counterflow diffusion flames by using the computer code employed in [6, 7]. The code allows the calculations of stretched laminar counterflow diffusion flames using complex thermal and transport properties, and a detailed reaction mechanism. Effects of sooting and radiation heat loss were neglected in this paper. The reaction scheme used is a C3 chemistry from reference 8, with the addition of Nitrogen chemistry from reference 9. Totally 50 species and 312 reactions were included.

The results from the solution of counterflow flames were transformed to those in mixture fraction space by solving the following equation:

$$\rho v \frac{dZ}{dx} = \frac{d}{dx}\left(\frac{\lambda}{c_p} \frac{dZ}{dx} \right) \tag{12}$$

with the boundary conditions of $Z=1$ at the fuel side and $Z=0$ at the oxidant side. Quantity λ is the thermal conductivity, c_p is the specific heat, and v is the local velocity of the mixture in a counterflow diffusion flame.

Turbulence Closure

The flow field was obtained by solving the general governing equations. The time average method [1] was employed. Turbulence was described by means of the standard $k-\varepsilon$ two-equation model [10]. The governing equations include those conservation equations of mass, momentum, turbulent kinetic energy ($\overline{k}$), dissipation rate of turbulence kinetic energy ($\overline{\varepsilon}$), mean mixture fraction $\overline{Z}$ and its variance ($\overline{g}$). These equations can be written as:

$$\frac{\partial}{\partial x_k}\left(\overline{\rho u}\right) = 0 \tag{13}$$

$$\frac{\partial}{\partial x_k}\left(\overline{\rho u_k u_i}\right) = \frac{\partial}{\partial x_k}\left[\mu_t \left(\frac{\partial \overline{u_i}}{\partial x_k} + \frac{\partial \overline{u_k}}{\partial x_i} \right) \right] - \frac{\partial}{\partial x_i}\left(p + \frac{2}{3}\overline{\rho k} + \frac{2}{3}\mu_t \frac{\partial \overline{u_l}}{\partial x_l} \right) \tag{14}$$

$$\frac{\partial}{\partial x_k}\left(\overline{\rho u_k k}\right) = \frac{\partial}{\partial x_k}\left(\frac{\mu_t}{\sigma_k} \frac{\partial \overline{k}}{\partial x_k} \right) + G - \overline{\rho \varepsilon} \tag{15}$$

$$\frac{\partial}{\partial x_k}\left(\overline{\rho u_k \varepsilon}\right) = \frac{\partial}{\partial x_k}\left(\frac{\mu_t}{\sigma_\varepsilon} \frac{\partial \overline{\varepsilon}}{\partial x_k} \right) + C_1 \frac{\overline{\varepsilon}}{\overline{k}} G - C_2 \overline{\rho} \frac{\overline{\varepsilon}^2}{\overline{k}} \tag{16}$$

$$\frac{\partial}{\partial x_k}\left(\overline{\rho Z}\right)=\frac{\partial}{\partial x_k}\left(\frac{\mu_t}{\sigma_Z}\frac{\partial \overline{Z}}{\partial x_k}\right) \tag{17}$$

$$\frac{\partial}{\partial x_k}\left(\overline{\rho u_k g}\right)=\frac{\partial}{\partial x_k}\left(\frac{\mu_t}{\sigma_g}\frac{\partial \overline{g}}{\partial x_k}\right)+C_{g1}\mu_t\left(\frac{\partial \overline{Z}}{\partial x_k}\right)-C_{g2}\overline{\rho}\frac{\overline{\varepsilon}}{\overline{k}}\overline{g} \tag{18}$$

$$G=\mu_t\left(\frac{\partial \overline{u_j}}{\partial x_k}+\frac{\partial \overline{u_k}}{\partial x_j}\right)\frac{\partial \overline{u_j}}{\partial x_k} \tag{19}$$

$$\mu_t=C_\mu \overline{\rho k}^2/\overline{\varepsilon} \tag{20}$$

The model constants used in the present paper are those commonly used in the literatures [1, 3, 10]. They are: $C_\mu=0.09$, $C_1=1.44$, $C_2=1.92$, $\sigma_k=1.0$, $\sigma_\varepsilon=1.3$, $\sigma_Z=0.9$, $\sigma_g=0.9$, $C_{g1}=2.8$ and $C_{g2}=2.0$.

A general-purpose multi-block 3-D code, FLEX [11], was employed to solve these governing equations. The standard wall function method was used for the near wall treatment. All the governing equations were discretized by the control volume method. The convective terms in the equations were discretized using the upwind scheme while the diffusion terms were discretized by center differencing scheme. Non-staggered grid arrangement was used. The SIMPLE algorithm [12] was employed to deal with the velocity and pressure coupling. The stone's method [13] was used to solve the discritized equations.

Since the combustion process affects the flow field through the density, only the integration of density $\overline{\rho}$ (by means of the equation 4) was carried out during the solution process of flow field. The computations of temperature and all other state quantities were obtained off-line after the flow field was determined. Therefore the computational cost can be greatly saved by flamelet model.

RESULTS AND DISCUSSIONS

Using the above flamelet model, the combustion and NO_X emission process of a gas turbine reactor was simulated. Figure 1 shows the geometry and dimensions of the modeled gas turbine combustor. The central fuel pipe radius is 4.20 mm. The inner and outer radius of the annular air port are 31.80 mm and 37.95 mm, respectively.

Due to the symmetry, only half the combustor was simulated in the cylindrical coordinate system. The inlet of the simulation domain was placed immediately above the fuel pipe exit. The inlet section was not included in the simulation domain. Figure 2 is the computational grid. Totally 2420 grids were used, with finer grids placed near the inlet region.

Both fuel (C_3H_8) and air enter the combustor at the temperature of 300 K. The inlet velocities of fuel stream are $\overline{u}$ = 19.0 m/s and $\overline{v}$ = 0.0, while those of air stream are $\overline{u}$ = 29.0 m/s and $\overline{v}$ = 10.5 m/s ($\overline{u}$ and $\overline{v}$ are respectively the mean axial and radial direction velocities). The inlet fuel and air stream densities are, respectively, 1.8 and 1.17 kg/m^3.

Radiation heat transfer and sooting process were neglected in the simulation.

In the following sections, we first discuss the profile of a single flamelet and the effect of stretch rate (scalar dissipation rate) on the flamelet. Then the simulation results for the model gas turbine combustor are given.

The Flamelet Profile

The flamelet library can be created either experimentally or computationally. In this paper, it was established by the numerical simulations of a series of adiabatic counterflow diffusion C_3H_8/air flames with different stretch rates. Radiation heat loss and sooting process were neglected.

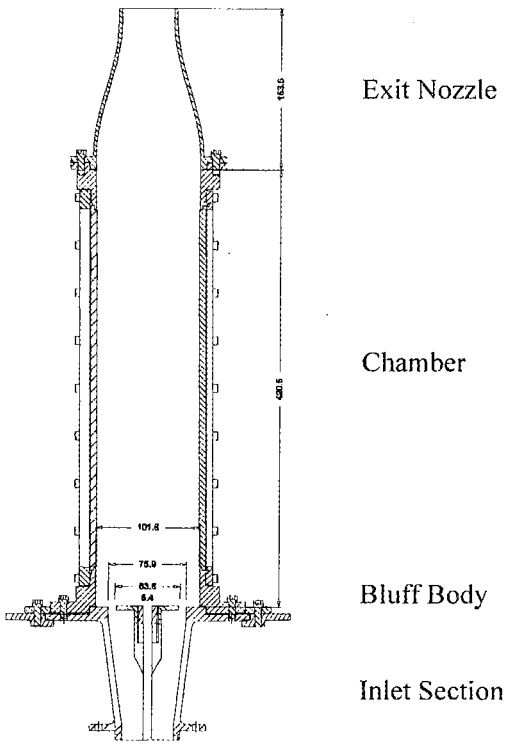

Fig. 1 The geometry of the model gas turbine Combustor

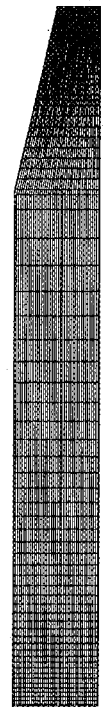

Fig. 2 Computational meshs

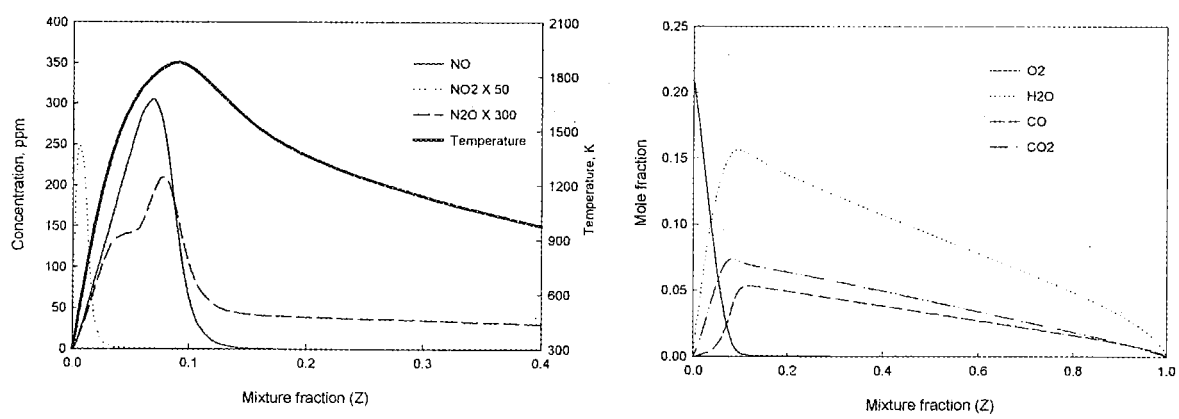

Fig. 3 Profiles of temperature, CO_2, CO, H_2O, O_2, NO, NO_2 and N_2O for the flamelet with stretch rate of 80 1/s.

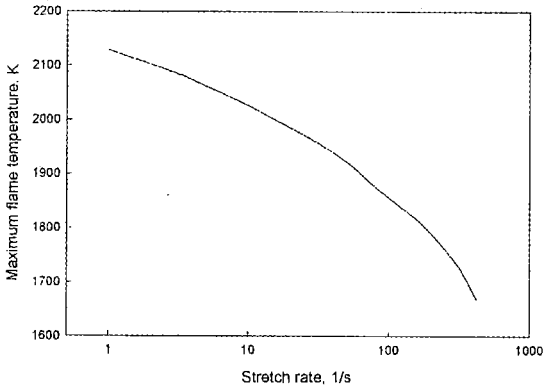

Fig. 4 The effect of stretch rate on maximum flame temperature

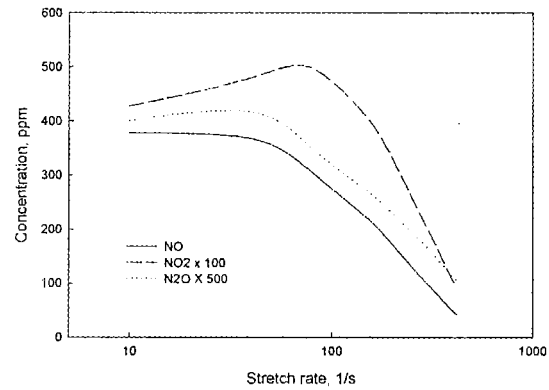

Fig. 5 The effect of stretch rate on maximum concentrations of NO, NO_2 and N_2O

Figure 3 gives the profiles of flame temperature and concentrations of CO, CO_2, H_2O, O_2, NO, NO_2 and N_2O in the mixture fraction space for the flame with the stretch rate of 80 s^{-1}, which corresponds to a scalar dissipation rate of 24.63 s^{-1}. It demonstrates that while the main combustion products (such as H_2O, CO and CO_2), NO and N_2O appear in the primary reaction zone (with higher temperatures), NO_2 appears in the region near the air side (Z = 0) where temperatures are relatively low. This is because that NO_2 is mainly produced by the reaction $HO_2+NO=NO_2+OH$. The activation energy of this reaction is negative, and HO_2 is always produced near the air side.

The profiles of temperature and species for the flamelets with other stretch rates are similar to those in Fig. 3, except that the absolute values are different.

The maximum temperatures of different stretch rate (or scalar dissipation rate) counterflow C_3H_8/air diffusion flames are shown in Fig. 4. It is noted that when stretch rate increases, the maximum flame temperature reduces and finally flame extinguishes at the stretch rate of 422.0 s^{-1}, corresponding to a scalar dissipation rate $\chi_{max} = 100.77\ s^{-1}$. The solution of counterflow diffusion flame does not exist if the stretch rate is higher than this critical value, named stretch extinction limit. Therefore the flamelet library has been created by the simulations of counterflow diffusion flames with stretch rates lower than the stretch extinction limit. The computations were conducted for twelve counterflow diffusion flames, corresponding to χ_{max}=0.12, 0.35, 0.73, 1.41, 5.13, 12.25, 24.63, 42.34, 60.19, 78.58, 91.23 and 100.77 s^{-1}. The simulations for further lower χ_{max} value were not performed, since the flame thickness sharply increases and then the flamelet model does not apply any more.

The maximum concentrations of NO, NO_2 and N_2O in counterflow flames at different stretch rates are shown in Fig. 5. They indicate that NO emission in the flame decreases with the stretch rate increase. This is due to the variation of flame temperature, as shown in Fig. 4. The variation of maximum N_2O concentration is similar to that of NO, since the main route for the production of N_2O is the reaction $NH + NO = N_2O + H$. However, the maximum concentration of NO_2 first increases to a peak value at the stretch rate of 80 s^{-1}, and then decreases with further increase in stretch rate. The increase of NO_2 concentration at lower stretch rates is due to the

drop of flame temperature. However with the further increase of stretch rate, the concentrations of both HO_2 and NO sharply decrease, which results in the reduction of NO_2 production rate.

Applying these profiles to the turbulent flame in the model gas turbine combustor, we can link the combustion and NO_X emission with the flow field.

Distributions of Velocity, Temperature and Various Species in the Combustor

Figure 6 is the predicted near-field velocity distribution in the combustor. Even at this relatively coarse grid, it is seen that the simulation result is reasonable. There are two main re-circulation zones in the combustor. One is located between the fuel and air jets, and the other

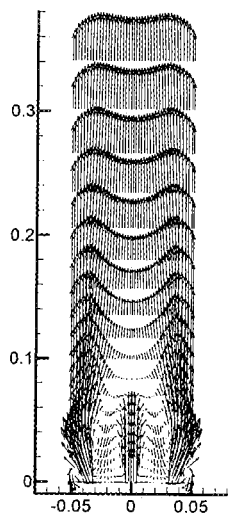

Fig. 6 Near-field velocity distribution

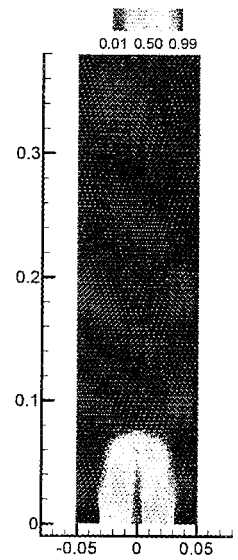

Fig. 7 Mole fraction distribution of fuel (C_3H_8)

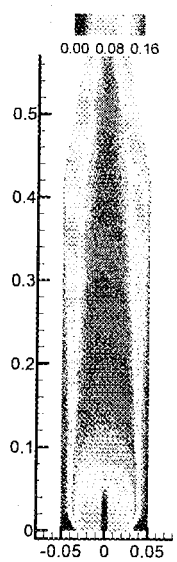

Fig. 8 Mole fractions of H_2O

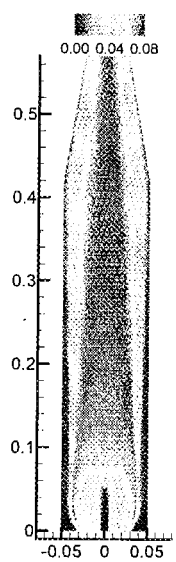

Fig. 9 Mole fractions of CO_2

between the air jet and combustor wall. These two zones help the ignition and flame stabilization in the chamber.

The predicted fuel (C_3H_8) concentration distribution is shown in Figure 7. It indicates that fuel is consumed within about 8 cm after entering the reactor.

Figures 8 and 9 demonstrate the distributions of main combustion products, H_2O and CO_2. They reveal that although the fuel is decomposed in the region below Z = 8.0 cm, the maximum concentrations of H_2O and CO_2 can not be reached until about Z equal to 12.0 cm on the axis. This is due to the existences of intermediate species, such as CO, H_2 etc.

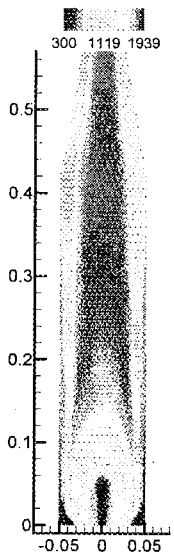

Fig. 10 Flame temperatures, K

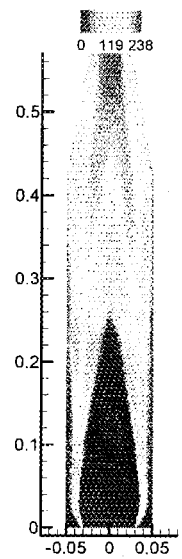

Fig. 11 Concentrations of NO, ppm

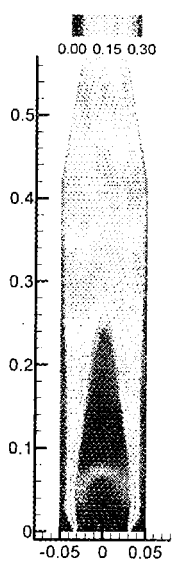

Fig. 12 Concentrations of N_2O, ppm

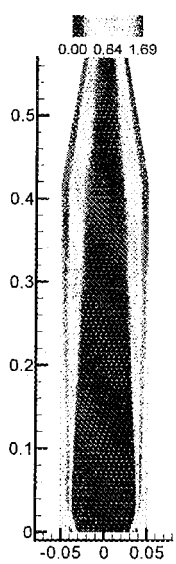

Fig. 13 Concentrations of NO_2, ppm

Figures 10-13 show the predicted flame temperatures and the concentrations of NO, NO_2 and N_2O in the combustor. As expected, NO mainly appears in the higher temperature region. It is because thermal mechanism dominates the production of NO, and the production rate of thermal NO depends on temperature and the super-equilibrium concentrations of O and OH that usually appear in the main reaction zone.

Similarly, the concentrations of N_2O also appear in the relatively higher temperature region. However, the concentrations of N_2O are much lower than those of NO.

Being different from NO, the concentrations of NO_2 in the higher temperature region are relatively very small. In contrast, higher levels of NO_2 occur outside the primary reaction zone. This is because NO_2 is mainly produced by the reaction $HO_2+NO=NO_2+OH$, and HO_2 is always produced outside the primary reaction zone.

The above results are qualitatively consistent with those experimentally measured. However quantitatively there are some differences, since radiative heat transfer and sooting have not been included in the current model. These effects will be implemented into the code in the future.

Even though, the results of this paper give a good local information of the zones where the main NO_X formation occurs and can be used to optimize the mixing pattern for minimizing NO_X production in the combustor. More importantly, by using a detailed chemistry model in establishing the flamelet library, this paper gives the separate production zones of NO, NO_2 and N_2O, which is usually difficult to obtain by most conventional models.

CONCLUSIONS

A numerical simulation of NO_X emission in a model gas turbine combustor has been carried out by means of stretched flamelet model. The simulation gives qualitatively reasonable result, although the radiative heat transfer and sooting effect have been ignored in the present model. The result is quite helpful for the understanding of NO_X emission during combustion process and the improvement of the design and operation of gas turbine combustor.

REFERENCES

1. Bilger, R.W., *Turbulent Reacting Flows* (Ed. by Libby, P.A., and Williams, F.A.), Springer-Verlag, Berlin, 1980.
2. Magnussen, B.F., and Hjertager, B.H., *Proc. Comb. Inst.* 6: 719 (1976).
3. Libby, P.A., and Williams, F.A., *Turbulent Reacting Flows*, Academic Press, New York, 1994.
4. Peters, N., *Prog. Energy Combust. Sci.* 10: 319-339 (1984).
5. Liew, S.K., Bray, N.C., and Moss, J.B., *Combust. Flame* 56:199-213 (1984).
6. Maruta, K., Yoshida, M., Guo, H., Ju, Y., and Niioka, T., *Combust. Flame* 112: 181-187 (1998).
7. Guo, H., Matovic, M.D., Becker, H.A., Sobiesiak, A., and Lawrence, A.D., *Proc. of the Combustion Institute/ Canadian Section 1998 spring technical meeting*, pp.6.21-6.25 (1998).
8. Stahl, G., and Warnatz, J., *Combust. Flame* 85:285-299 (1991).

9. Miller, J.A., and Bowman, C.T., *Prog. Energy Combust. Sci.* 15: 287-338 (1989).
10. Launder, B.E., and Spalding, D.B., *Comp. Methods Appl. Mech. Eng.*3:269 (1981).
11. Matovic, D.M., Solver Performance at Non-Matching Interface, CFD2000 conference, Montreal, June 11-13, 2000.
12. Patankar, S.V., *Numerical Heat Transfer and Fluid Flow*, Hemisphere, New York, 1980.
13. Stone, H.L., Siam J. Num. Anal. 5: 530-558 (1968).